POLITECNICO
MILANO 1863

SCUOLA DI INGEGNERIA INDUSTRIALE
E DELL'INFORMAZIONE

Executive Summary of the Thesis

Development and Testing of STASIS Balancing Algorithm

Laurea Magistrale in Space Engineering - Ingegneria Spaziale

Author: Niccolò Giannone

Advisor: Prof. Francesco Topputo

Co-advisor: Gianfranco Di Domenico, Dr. Gianmario Merisio

Academic year: 2022-2023

1. Introduction

In the dynamic field of space exploration, CubeSats have emerged as a cost-effective and efficient solution, revolutionizing practices in the access to space. However, the rapid growth in their deployment has outpaced the development of spacecraft communication systems, presenting a unique challenge. The ERC-funded Engineering Extremely Rare Events in Astrodynamics for Deep-Space Missions in Autonomy (EXTREMA) project is poised to bridge this gap by enhancing CubeSats with advanced autonomous capabilities, thus reducing reliance on traditional communication methods. To realize this ambitious vision, the project is anchored on three fundamental pillars.

1. **Autonomous Navigation**: Developing advanced navigation algorithms that enable CubeSats to autonomously determine their position in deep-space, leveraging the surrounding environment.
2. **Autonomous Guidance and Control**: Implementing efficient, lightweight guidance algorithms tailored to the computational limitations of CubeSats, enabling precise, time-defined thrust profiles.
3. **Ballistic Capture**: Exploiting the multi-body dynamics of the Solar System to maintain prolonged proximity to celestial bodies.

The success of EXTREMA hinges on the reliability of its GNC algorithms. Hence, rigorous testing to assess performances and robustness is paramount, ensuring the project not only meets but exceeds the rigorous demands of space exploration. EXTREMA stands as a testament to human ambition, paving the way for a new era in CubeSat technology and its applications in the vast expanse of space.

1.1. STASIS

To establish a solid foundation for research progress and risk mitigation, particularly relevant in cutting-edge projects as EXTREMA, a specialized CubeSat simulator, SpacecrafT Attitude SImulation System (STASIS) [1], was developed at the Deep-space Astrodynamics Research and Technology (DART) laboratory of the Polytechnic of Milan. In the technical setup, the platform is positioned atop a spherical bearing air joint, tailored to produce a thin film of air, thus creating a quasi friction-less environment for the platform above. STASIS primary objective is to serve as a ground-based testing platform for autonomous GNC algorithms. As a consequence, STASIS shall accurately mimic the attitude trajectory of deep-space probes. How-

ever, a considerable challenge emerges at this instance. STASIS, incapable of replicating a micro-gravity trajectory in its exact form, requires meticulous design to accomplish this goal.

1.2. The balancing problem

The primary distinction between the attitude trajectory in space and on the ground stems from the effect of gravitational torques. Contrasting with deep-space probes that rotate around their Centre of Mass (CM), the Centre of Rotation (CR) for STASIS is inherently constrained due to its mechanical arrangement. However, as evident from rigid body equations,

$$J\dot{\boldsymbol{\omega}} = J\boldsymbol{\omega} \times \boldsymbol{\omega} + m\mathbf{g} \times \mathbf{r}_{CM} + \mathbf{M} \qquad (1)$$

wherein,

J	Inertia tensor
$\boldsymbol{\omega}$	Angular velocity vector
m	Total mass
$\mathbf{g}$	Gravity vector
$\mathbf{r}_{CM}$	CR-CM offset
$\mathbf{M}$	External disturbance torque

if the internal mass distribution of the system is strategically altered to cancel the CR-CM offset, the testbed can effectively mirror the attitude behavior of a deep-space probe.
To adeptly cancel the CR-CM offset, STASIS is equipped with a system of eight stepper-motor-driven masses, as illustrated in Figure 1. These actuators are distributed with two on each of the two in-plane axes and four along the vertical axis. While STASIS boasts these advanced actuation capabilities, it lacks of a corresponding algorithm sophisticated enough to command these masses effectively. Addressing this gap is the cornerstone of this work.

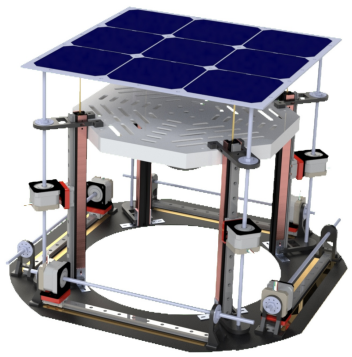

Figure 1: 3D rendering of STASIS.

2. The experiment pillars

To ensure uniformity in the experimental setup, three principles for the algorithm were defined.

1. **Adaptability**: The algorithm must be designed to function seamlessly with an evolving platform, negating dependence on CAD data that could be invalidated by any modification in the satellite mock-up.
2. **Compatibility**: The algorithm needs to efficiently function within the constraints of the existing hardware setup, which, at the time of the experiment, does not include reaction wheels.
3. **Precision**: The algorithm should strive for the highest achievable accuracy.

These pillars were fundamental in establishing the high-level requirements that guided the design process.

3. Balancing algorithms

Excluding human-in-the-loop procedures, three distinct categories of methods for platform balancing can be delineated:

- An *open-loop* approach, which operates based on pre-acquired CAD data for the precise allocation of masses.
- An *observe-and-compensate* approach, entailing empirical data acquisition of platform kinematics to subsequently infer and correct the CR-CM offset.
- A *closed-loop* schema, leveraging a dynamic control algorithm that directs the masses towards a state wherein the offset is intrinsically nullified.

Setting aside the open-loop approaches, which inherently conflict with the experiment's flexibility criterion, the remaining methods were rigorously examined. The overarching goal was to amalgamate different strategies, sidestepping the implicit limitations of each while capitalizing on their strengths.

3.1. Observe-and-compensate

In the observe-and-compensate framework, the core concept involves executing optimization algorithms that calibrate the unknown parameters using a predefined mathematical model. Within this approach, presuming prior knowledge of inertia parameters turns out to be a significantly limiting assumption, typically resulting in sub-

optimal outcomes. Consequently, incorporating the inertia tensor into the estimation process becomes a viable solution.
However, the integration of inertia parameters into the estimation process, while beneficial for accuracy, introduces complexities related to observability. Indeed, being $\mathbf{x}$ the real solution of the problem,

$$\mathbf{x} = [\tilde{\mathbf{J}}\ \mathbf{r}_{CM}]^T \tag{2}$$

with,

$$\tilde{\mathbf{J}} = [J_x\ J_y\ J_z\ J_{xy}\ J_{xz}\ J_{yz}]^T, \tag{3}$$

any scaling $\alpha\mathbf{x}$ of the real solution, yields identical sensor outputs as the real solution, since,

$$\begin{aligned}\dot{\boldsymbol{\omega}} &= \frac{J^{-1}}{\alpha}(-\boldsymbol{\omega} \times \alpha J\boldsymbol{\omega} - m[\mathbf{g}\times]\alpha\mathbf{r}) \\ &= \frac{J^{-1}}{\alpha}\alpha(-\boldsymbol{\omega} \times J\boldsymbol{\omega} - m[\mathbf{g}\times]\mathbf{r}) \\ &= J^{-1}(-\boldsymbol{\omega} \times J\boldsymbol{\omega} - m[\mathbf{g}\times]\mathbf{r}).\end{aligned} \tag{4}$$

To re-establish observability within the problem, two potential strategies may be implemented:

- Utilizing actuators to generate a torque in the tridimensional space.
- Implementing a mathematical constraint on the unknown vector to address the problem of homothety.

At this juncture, the considerable complexity inherent in the experiment design becomes more apparent. Deriving inertia parameters from CAD data would contravene the principle of flexibility; implementing reaction wheels could breach the compatibility one; and introducing a mathematical constraint might render the problem susceptible to error propagation, potentially undermining precision. Therefore, conducting a preliminary numerical simulation to gauge the achievable results, followed by a thorough analysis, is a crucial phase to amalgamate the design pillars of the procedure.

3.2. Closed-loop approach

The rationale underlying the methodology is to devise a control law that steers the stepper-motor-driven masses towards a configuration in which the offset is neutralized. This achievement can be realized through direct estimation of the offset, or imposing a condition (e.g., null angular momentum), wherein intrinsically the offset must have settled to zero.

Hence, following the implementation of the feedback law to impart, it is necessary to translate the command into specific directives for the mass actuators. To fulfill this objective, the torque generated the individual actuator is inspected:

$$\boldsymbol{\tau}_u = m_i(-\mathbf{g} \times \mathbf{R}_i),\ i = 1 \dots 8. \tag{5}$$

wherein,

$\boldsymbol{\tau}_u$	Control torque
m_i	Actuation system mass
$\mathbf{g}$	Gravity vector
$\mathbf{R}_i$	Actuation system position vector

As discernible from Equation (5), the torque generated by the actuators is constrained to a plane orthogonal to the gravity vector. This leads to two significant implications:

- The control problem is under-actuated, precluding the capability to counterbalance the offset in three-dimensional space.
- The control law must be structured to be in the range of $[-\mathbf{g}\times]$, ensuring its consistency with the torque generation capabilities of the actuators.

Despite the inherent non-invertibility arising from the singularity of matrix $[-\mathbf{g}\times]$, Equation (5) always yields a solution for $\mathbf{R}_i$ if the control is consistently generated.

$$\mathbf{R}_i = \frac{\mathbf{g} \times \boldsymbol{\tau}_u}{||\mathbf{g}||^2 m_i}. \tag{6}$$

In defiance of the operational complexity associated with online wireless actuation, the implementation of closed-loop methods could significantly enhance the compensation process. Through careful mathematical structuring, these methods are well-suited to fulfill the project's foundational pillars. Indeed, their proficient environmental robustness, capability to operate without the need for preliminary estimations or external control, and demonstrated precision, collectively position them as a valuable asset in this context.

3.3. Methodologies amalgamation

The analysis undertaken lays the groundwork for outlining an initial framework of the experiment that aligns with the core pillars of the design process. Specifically, a strategy that integrates an active control technique to impose a

mathematical constraint within an observe-and-compensate methodology appears to satisfactorily adhere to the adaptability and compatibility criteria of the project. However, to ascertain whether this approach can theoretically meet the precision pillar, a robust foundation of simulation is essential.

4. Digital twin simulations

Extensive simulations conducted using the platform's digital twin validated the effectiveness of the implemented algorithms. This process greatly expedited the identification and understanding of the primary sources of error in the balancing problem, providing valuable insights for refinement and optimization.

4.1. Closed-loop simulations

To optimize the experiment to its fullest potential, a comprehensive set of algorithms was subjected to simulation, with the primary goal of selecting the most effective one. This step is critical to minimize the impact of error propagation through the mathematical constraints imposed on the subsequent observer. Namely, the simulated techniques were:

1. a PID control, exploiting the platform Euler angles for feedback;
2. a $\hat{\mathbf{g}}$ control, based on the knowledge of the local vertical direction to stabilize horizontally the platform [2];
3. a $\mathbf{H}$ control, tailored to conserve the platform angular momentum [3];
4. a $\tilde{\mathbf{r}}$ control, fed with a time-integration of a preliminary offset estimation [4].

The control torque is mapped into an actuator command, resulting in the residual values as outlined in Table 1.

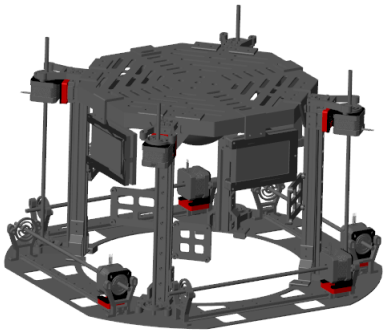

Figure 2: Digital twin CAD assembly.

Table 1: Closed-loop residual evaluation over 600 s simulations on the platform digital twin, upon incorporation of noise and drag.

Methods	r_x [m]	r_y [m]
PID control	$\sim 10^{-6}$	$\sim 10^{-6}$
$\hat{\mathbf{g}}$ control	$\sim 10^{-7}$	$\sim 10^{-7}$
$\mathbf{H}$ control	$\sim 10^{-4}$	$\sim 10^{-4}$
$\tilde{\mathbf{r}}$ control	$\sim 10^{-4}$	$\sim 10^{-4}$

Despite the theoretical effectiveness of each methodology, Table 1 reveals that two approaches exhibit divergence under conditions where sensor noise and aerodynamic damping effects are factored into the simulations. This complexity was thoroughly investigated, tracing the issue back to certain internal phases of the control processes, wherein error aggregation was observed. Conversely, PID and $\hat{\mathbf{g}}$ control laws were observed suitable for the application, due to their implicit segregation of the corrupted measurements in the inner loop.

4.2. Observe-and-compensate

Upon strategical rearrangement of rigid body equations, the problem can be written as:

$$\mathbf{\Omega x} = \mathbf{0} \tag{7}$$

with,

$$\mathbf{\Omega}(\dot{\boldsymbol{\omega}}, \boldsymbol{\omega}, \mathbf{g}, m) = \begin{bmatrix} \dot{\omega}_x & \omega_y\omega_z & -\omega_x\omega_y \\ -\omega_y\omega_z & \dot{\omega}_y & \omega_x\omega_y \\ \omega_y\omega_z & -\omega_x\omega_z & \dot{\omega}_z \\ \dot{\omega}_y - \omega_x\omega_z & \dot{\omega}_x + \omega_y\omega_z & \omega_x^2 - \omega_y^2 \\ \dot{\omega}_z + \omega_x\omega_y & \omega_z^2 - \omega_x^2 & \dot{\omega}_x - \omega_y\omega_z \\ \omega_y^2 - \omega_z^2 & \dot{\omega}_z - \omega_x\omega_y & \dot{\omega}_y + \omega_x\omega_z \\ 0 & g_z m & -g_y m \\ -g_z m & 0 & g_x m \\ g_y m & -g_x m & 0 \end{bmatrix}^T, \tag{8}$$

$$\mathbf{x} = [\tilde{\mathbf{J}}\ \mathbf{r}_{CM}]^T \tag{9}$$

Hence, collecting multiple samples, a matrix encompassing all the N measures $\mathbf{\Omega}_N$ is constructed, enabling to a constrained least square fitting of the dynamics equations, formally structured as:

$$\text{Find } \mathbf{x}^* \text{ s.t.} \begin{cases} ||\mathbf{\Omega}_N \mathbf{x}^*|| \text{ is minimized} \\ B\mathbf{x}^* = \mathbf{c} \end{cases} \tag{10}$$

wherein the mathematical constraint is retrieved through the active control methodology,

$$\underbrace{\begin{bmatrix} 0_{1\times 6} & 1 & 0 & 0 \\ 0_{1\times 6} & 0 & 1 & 0 \end{bmatrix}}_{B} \mathbf{x}^* = \underbrace{\begin{bmatrix} r_x \\ r_y \end{bmatrix}}_{\mathbf{c}}. \tag{11}$$

Equation (10) is integrated to circumvent the inaccuracies that may arise from the noisy angular accelerations obtained via numerical differentiation. Furthermore, to optimize performance, the measurements are subjected to a Savitzky-Golay filtering process. Despite these measures, the method exhibits limited accuracy, as evident from Table 2. An alternative strategy involves utilizing the available inertia parameters within a Kalman filter to refine the compensation of the vertical offset. The logic underpinning this approach is twofold: firstly, batch estimation, while robust against unmodeled effects, typically does not deliver exceptionally precise results. Conversely, the Kalman filter, though capable of attaining high accuracy levels, exhibits considerable sensitivity to unmodeled effects. Table 2 indicates that the unscented Kalman filter, even when provided with biased inertia parameters derived from the least squares estimation, theoretically possesses the capability to enhance the accuracy of r_z estimation.

Table 2: Observe-and-compensate residual evaluation across different methods, upon incorporation of noise and drag.

Methods	r_x [m]	r_y [m]	r_z [m]
Least squares	-	-	$\sim 10^{-4}$
LSQ→EKF	$\sim 10^{-5}$	$\sim 10^{-6}$	$\sim 10^{-4}$
LSQ→UKF	$\sim 10^{-5}$	$\sim 10^{-5}$	$\sim 10^{-5}$

5. The experiment

Following months of dedicated research, the algorithm is tested on STASIS. The procedure is intrinsically composed of 2 steps:

1. an active control technique to perform the planar balancing procedure;
2. a state observation to provide the residual offset estimation, potentially enhanced through Kalman filtering.

Theoretically, to achieve a consistent mathematical constraint (i.e, $\mathbf{c} \neq [0\ 0]^T$), it is necessary for the masses to be relocated from their equilibrium position to initialize the second phase of the procedure. This adjustment exposes the procedure to relevant risks, including human operational errors and the potential for the stepper motors to skip steps. For instance, conjecturing that 50 steps are missed during a 60000-step command, the error introduced would be on the order of 10^{-5} m. Such an error magnitude is two orders greater than the theoretical precision that the active control system is capable of achieving. Hence, the experiment was re-conceptualized to be performed in a single operational phase. The essential idea of this procedural condensation lays in designing an experiment where a unique initialization stands for both the subsequent steps. As depicted in Figure 3, the system undergoes a preliminary observational phase before the initiation of the control law. The data collected during this phase, along with the imposed mathematical constraint, will be instrumental for the post-processing determination of the vertical offset.

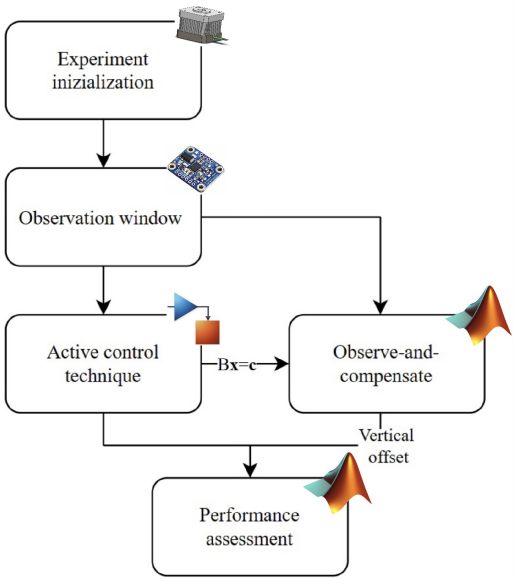

Figure 3: Schematic representation of experiment phases.

Contrarily, the active control law is applied real-time via Simulink. Three different protocols are employed to manage the communication with sensor and actuators:

- HTTP for the request-respond mechanism of the attitude reconstruction software;
- TCP for the communication with the inertial measurement unit;
- UDP to send the online commands to the

actuators controllers.

5.1. Results

As illustrated in Figure 4, on the day of the experiment, STASIS was outfitted solely with two masses, precluding the capability for tridimensional compensation of the platform.

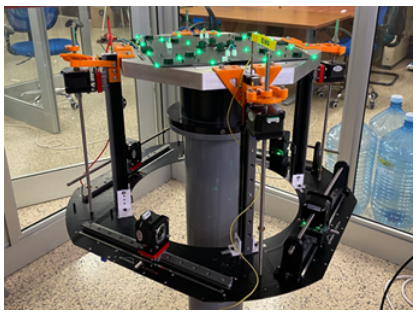

Figure 4: STASIS the day of the first experiment, wherein the light-emitting masses are the active ones.

The active control approach is designed to function at two separate frequencies due to the different capabilities of the hardware used for attitude determination and control. Attitude reconstruction is optimized at 10 Hz to prevent from request throttling, while actuation processes are set to the lower frequency of 1 Hz.
The PID control test was prematurely terminated when the wireless connection to the attitude reconstruction server was lost, indicatively 820 seconds post-initialization. Figure 5 presents the Euler angles history during the control, proving its efficacy to compensate the Cubesat simulator.

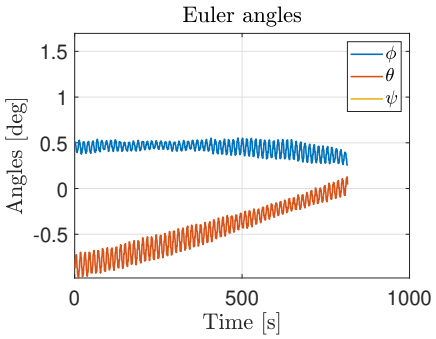

Figure 5: Euler angles history during PID.

A static analysis of the Euler angles indicated a residual offset of:

$$\begin{aligned} r_x &\sim 10^{-6} \text{ m}, \\ r_y &\sim 10^{-5} \text{ m}. \end{aligned} \tag{12}$$

The nonlinear control method was also executed. During the control phase, however, a malfunction occurred with one mass. The mass remained stuck due to a structural discontinuity on STASIS, leading to jamming and repetitive erroneous command for the pitch-oriented mass, as illustrated in Figure 6. This issue caused the experiment to be artificially halted after 330 s.

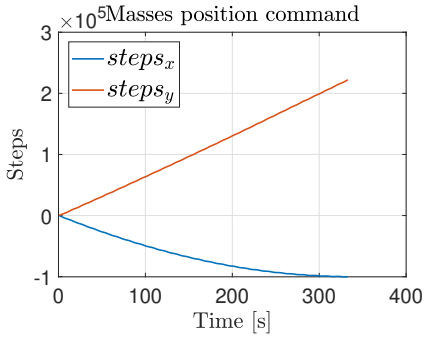

Figure 6: Integrated mass command during the non linear $\hat{\mathbf{g}}$ control.

6. Conclusions

Despite the setbacks encountered in the experiments, the findings lay a solid foundation for the future automatic balancing of STASIS. Notably, the PID control revealed its capabilities to compensate the platform in a feasible timeframe. Concerning the non-linear control actuation, while one mass experienced jamming, another successfully reached an equilibrium point, offering valuable insights.
This work not only demonstrates the feasibility of balancing STASIS but also provides preliminary operational parameters, including optimal gains and working frequencies that avoid system throttling and ensure timely compensation.
For future iterations, addressing the structural discontinuity in the linear guide, which led to the jamming of the mass, is paramount. With this modification, it is advisable to proceed with the current methodology. This approach has shown considerable promise, exhibiting robustness and adaptability in the face of the complexities typical of real-world experiments.

References

[1] G. Di Domenico and F. Topputo. STASIS: An Attitude Testbed for Hardware-in-the-Loop Simulations of Autonomous Guidance, Navigation, and Control Systems. In *73rd International Astronautical Congress (IAC 2022)*, pages 1–20, 2022.

[2] Anton Bahu and Dario Modenini. Automatic mass balancing system for a dynamic CubeSat attitude simulator: development and experimental validation. *CEAS Space Journal*, 03 2020. doi: 10.1007/s12567-020-00309-5.

[3] Jae Jun Kim and Brij N. Agrawal. Automatic Mass Balancing of Air-Bearing-Based Three-Axis Rotational Spacecraft Simulator. *Journal of Guidance, Control, and Dynamics*, 32(3):1005–1017, 2009. doi: 10.2514/1.34437.

[4] Simone Chesi, Qi Gong, Veronica Pellegrini, Roberto Cristi, and Marcello Romano. Automatic Mass Balancing of a Spacecraft Three-Axis Simulator: Analysis and Experimentation. *Journal of Guidance, Control, and Dynamics*, 37(1):197–206, 2014. doi: 10.2514/1.60380.